Separation and Purification Technology 286 (2022) 120430

Contents lists available at ScienceDirect

Separation and Purification Technology

journal homepage: www.elsevier.com/locate/seppur

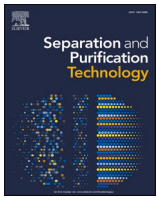

Recovery of bio-based medium-chain fatty acids with membrane filtration

Stewart Charles McDowall, Maria Braune, Roy Nitzsche *

DBFZ Deutsches Biomasseforschungszentrum gemeinnützige GmbH, Torgauer Straße 116, 04347 Leipzig, Germany

ARTICLE INFO

Keywords:
Biorefinery
Fermentation broth
Medium-chain fatty acids
Ultrafiltration
Nanofiltration

ABSTRACT

Medium-chain fatty acids (MCFAs) are promising platform chemicals for biorefineries in the circular economy. An efficient and sustainable process for their recovery from biomass, however, remains elusive. This work aimed to develop a separation cascade for MCFA recovery from fermentation broth (FB) using membrane filtration. This technical-scale process consisted of a filter-press, thermal-pretreatment, ultrafiltration (UF), and nanofiltration (NF). While solid–liquid separation and UF were efficient, NF fluxes declined rapidly due to membrane fouling, limiting MCFA separation and concentration. Thermal pretreatment and UF membrane pore size had a negligible effect on filtration performance and diafiltration trials in NF proved ineffective. While process feasibility is presently constrained by membrane fouling in NF, characterization, and reduction of foulants could make the process readily viable. Overall, the membrane filtration cascade yielded a product, the NF retentate, with an MCFA concentration approximately 230% greater than that of the feedstock with an average overall recovery of 84%. Furthermore, although the concentration of MCFAs (C4-C8, 12.9 g L^{-1}) may be inadequate for direct use, this product, being clarified and enriched, could serve as an improved feedstock for MCFA purification by alternative methods.

1. Introduction

The imperative transition to a sustainable, bio-based, circular economy is gaining momentum. Central to this new paradigm is biomass, and it is crucial that a large variety of processes are developed for its valorization in biorefineries [1].

In Germany, the development of integrated biorefineries has gained particular significance due to the impending expiration of biogas subsidies. While >9000 biogas facilities provide an important source of baseload electricity, low gas prices and reduced tariffs are predicted to make them rapidly uneconomical [2]. The future of this sector, therefore, depends on diversification and value addition by retrofitting existing biogas plants to become biorefineries that can create a variety of more profitable products from biomass [3]. To this end, the co-production of medium-chain fatty acids (MCFAs) and biogas has been identified as a promising synergy, whereby existing biogas facilities could be adapted to include separation technologies for the recovery of MCFAs from the digestate. Both the fermentation and separation processes are under intensive study [4].

Currently, MCFAs are obtained industrially as a byproduct of palm- and coconut-oil production, a process which is limited in scale and also controversial, due to negative externalities of expanding oil crop cultivation in tropical ecosystems [5]. MCFAs have a multitude of applications and given a sustainable and efficient source, have the potential to become an important new class of bio-based platform chemicals [6]. As an alternative to extracting MCFAs from tropical oil crops, a biochemical process called mixed-culture chain elongation (MCCE) has been established to produce them from biomass [7]. From such MCCE processes, however, the combined MCFA concentration in the fermentation broth (FB) is typically limited to approx. 10 g L^{-1}, which can make downstream processing challenging and cost-intensive [4]. This study focuses on the development of a process for their recovery from the fermentation broth (FB) produced by the MCCE of maize silage. There are many possibilities for efficiency gains in recovery through innovation and optimization, and this is especially pertinent because downstream processes are often responsible for a significant proportion of the cost of bio-based products [8,9].

Abbreviations: COD, chemical oxygen demand; DF, diafiltration; DM, dry matter; EC, electrical conductivity; FA, fatty acid; FB, fermentation broth; GC, gas chromatography; MCCE, mixed-culture chain elongation; MCFA, medium-chain fatty acid; MF, microfiltration; MWCO, molecular weight cut-off; NF, nanofiltration; pKa, acid disassociation constant; PWF, pure water flux; RIS, resistance-in-series; RO, reverse osmosis; TMP, transmembrane pressure; UF, ultrafiltration; VFA, volatile fatty acid; VPMC, vapor pressure membrane contactor; VR, volume reduction.

* Corresponding author.
E-mail address: roy.nitzsche@dbfz.de (R. Nitzsche).

https://doi.org/10.1016/j.seppur.2021.120430
Received 22 June 2021; Received in revised form 30 December 2021; Accepted 30 December 2021
Available online 5 January 2022

Nomenclature

A	membrane surface area (m^2)
C_f	concentration feed ($g\ L^{-1}$)
C_p	concentration permeate ($g\ L^{-1}$)
J	volumetric flux ($L\ m^{-2}h^{-1}$)
J_{PWF}	pure water flux ($L\ m^{-2}h^{-1}$)
k_w	hydraulic permeability ($L\ s^{-2}\ bar^{-1}$)
m	mass (g)
MW	molecular weight (Da or $g\ mol^{-1}$)
P	pressure (bar)
P_{TMP}	transmembrane pressure (bar)
$R_{a/p}$	adsorption/pore blockage resistance (m^{-1})
R_{cp}	concentration polarization resistance (m^{-1})
R_f	fouling resistance (m^{-1})
$R_{g/c}$	gel/cake layer resistance (m^{-1})
R_{irr}	irremovable membrane resistance (m^{-1})
R_m	membrane resistance (m^{-1})
R_{obs}	observed rejection (%)
R_{tot}	total resistance (m^{-1})
Re	Reynolds number (-)
s	sample standard deviation
t	time (s)
T	temperature (°C)
v	crossflow velocity ($m\ s^{-1}$)
V	volume (L)
VR	volume reduction (-)
w_{DM}	dry matter (% (w/w))
μ	population mean
η	dynamic viscosity ($kg\ m^{-1}\ s^{-1}$)
σ	population standard deviation
$\overline{X}$	sample mean

Recovery of MCFAs can be achieved either directly from the bioreactor during fermentation, or by batch-wise treatment of the FB [10]. Direct extraction has the advantage that product-inhibition effects on the bacteria are minimized but presents additional challenges as the separation process must not inhibit the sensitive biosynthesis in MCCE. An early example of direct extraction is the *in situ* biphasic reactive extraction of fatty acids (FAs) using trialkyl phosphates, and while MCFA concentrations of up to 32 $g\ L^{-1}$ were achieved, many of these studies were limited in scale (<1 L) and often used expensive or hazardous solvents [11,12]. More recent methods have used pertraction (membrane aided extraction), which is advantageous because it avoids contact between the extracting agents and the biomass [13,14]. One promising approach, using a combination of in-line pertraction and membrane electrolysis, exploits the low solubility of associated C6 and C8 FAs (10.3 $g\ L^{-1}$ and 0.79 $g\ L^{-1}$) and pH control to continuously produce an oil containing 53% hexanoic acid and 37% octanoic acid [15]. This system, based on a liquid by-product of the corn-to-ethanol industry, is being intensively developed, and while proven to be moderately stable and effective, it remains complex and energy-intensive. A further limitation of this process is that it would likely require additional solid–liquid separation steps to handle other types of biomass, which often have a much higher solids loading. A further technology that is gaining increased attention is extraction with vapor permeation membrane contactors (VPMC) [16]. In this method, the driving force of separation is concentration gradient between two aqueous phases which are separated by a gas permeable membrane. With the use of an alkaline permeate phase, this technique can be selective for volatile acids, which will be directly deionized after diffusing through the membrane in their protonated form. In doing so, the concentration gradient that drives the separation can be maintained, since the volatile acids' partial pressure will always be higher in the more acidic feed. In one study, separation efficiencies of up to 95% of C3-C6 FAs were achieved at a laboratory scale using a variety of FB feeds that had been first acidified (pH < 4) and centrifuged [17]. In another study, the VPMC method was further developed by the introduction of an integrated leach-bed fermentation and membrane separation system for recovering VFAs from municipal solid waste [18]. This direct recovery system was shown to improve overall VFA production by 42%, demonstrating the advantage of concurrently removing these potentially cytotoxic fermentation products. Considering the literature overall, despite some promising results in studies on bio-based MCFA recovery, the scalability and economic viability of these processes are yet to be confirmed and further development is clearly necessary [10].

Although membrane filtration is an established industrial separation technique, its application to the purification of FB often presents serious challenges due to fouling on the membrane surface [19]. FB is especially difficult to filter because it is a complex and often undefined mixture that includes cells, proteins, lipids, polysaccharides, and salts. The identification of appropriate membranes and suitable procedures for their maintenance adds further complexity to the system design.

While no studies have been published concerning the successful recovery of concentrated MCFAs from FB with pressure-driven membrane filtration, lessons can be taken from similar processes with other low molecular weight (MW) carboxylic acids. A variety of multi-step recovery methods have been reported for succinic acid and lactic acid, often including a microfiltration (MF) step for FB clarification followed by NF for purification and reverse osmosis (RO) for concentration by dewatering [20–22]. These methods are yet to be proven at a full scale and, despite an efficient biosynthesis of the acids, their separation is still considered a bottleneck in production, accounting for >50% of costs [23]. While volatile fatty acids (VFAs) such as butanoic acid are most similar to MCFAs in terms of functionalization and acidity, they are smaller and more polar, which can lead to considerable differences in NF retention. The multifaceted transport mechanism in NF makes the retention behavior of membranes difficult to predict, though it has been found that hydrophobicity and a high negative surface charge favor the retention of butanoic acid [24]. The retention of VFAs by NF increases with pH due to charge repulsion effects, though size exclusion is also a factor, as differences have been reported between the retention of C2 and C4 FAs [25]. In one study with biogas hydrolysate, FAs ≥ C4 were concentrated up to a factor of 19 with several NF and RO membranes, though this was in a dead-end stirred-cell filtration unit [26]. Pretreatment of the feed by UF (10–50 kDa) was shown here to reduce membrane fouling and increase permeate flux in the subsequent filtrations.

With careful selection of the membranes and process conditions, it should be possible to direct the FAs to the desired filtration stream and even to fractionate the FAs based on chain length [16]. Given their pKa values of approximately 4.9, >90% of the FAs will be dissociated at a pH > 6 and should, therefore, be mostly retained by negatively charged membranes. Alternatively, by using a lower pH or a positively charged membrane the acids could permeate the NF filter and be subsequently concentrated by RO, though the additional step would likely increase costs [27].

There are several critical gaps in the literature concerning the effects of pretreatment, process parameters, and membrane selection with respect to permeate flux, fouling, and MCFA rejection. This study aims to improve our understanding of these factors, which are crucial to the development of an efficient and scalable process for the recovery of MCFAs from FB. The objectives are to (1) achieve an efficient solid–liquid separation by implementing a two-step filtration process

consisting of a filter press and a ceramic UF membrane, (2) examine the effects of UF pore size and thermal pretreatment on NF performance, and (3) concentrate the MCFAs in the NF retentate such that they can be easily purified.

2. Materials and methods

2.1. Materials

2.1.1. Fermentation broth

The FB used in this study was obtained from laboratory-scale MCFA-producing bioreactors based on a substrate of maize silage which was fermented in a semi-continuous anaerobic mixed-culture chain-elongation (MCCE) process. The fermentation was supplemented daily with trace elements, urea, and NaOH for pH control. The FB was removed periodically in 3–6 L batches from the 20 L reactors and stored at 4 °C. Details of the concentration and properties of the main FAs found in the FB are listed in Table 1. The FB was supplied by collaborators from the Helmholtz Center for Environmental Research (UFZ, Leipzig, Germany). Detailed information concerning the fermentation process has been published [28,29].

2.1.2. Membranes

For UF, multi-channel, tubular, ceramic, membranes from the manufacturer atech innovations (Germany) were used. The membrane units were 1178 mm long and contained seven 6 mm diameter channels. For NF, the high-rejection composite polymer TriSep TS80 membrane from Microdyn Nadir (USA) was used (cut into two 20 cm diameter flat sheets). Details of the UF and NF membranes according to the manufacturers are listed in Table 2.

2.1.3. Crossflow filtration system

The crossflow filtration system used during the experiments was a PiloMemI apparatus from PS Prozesstechnik GmbH (Switzerland) (Fig. 1). The FB in the temperature regulated feed tank (B01) was passed over the membrane (M01) and the retentate was returned to the tank through the heat exchanger (W01). Feed side pressure was regulated by adjusting the pump power (P01) and the post-column valve (V05). The transmembrane pressure (TMP) was set by adjustment of the permeate-side valve (V08). In total recirculation mode, the permeate was returned directly to the feed tank, whereas in concentration mode it was collected in containers. Flow rate measurements from FIR02 were verified gravimetrically by periodically weighing the collected permeate. The UF membranes were installed in the internal housing, whereas the NF membranes were installed in an external plate-and-frame module, the LabStak M20 from Alfa Laval (Sweden).

Process parameters were selected based on results from previous NF screening experiments [30]. For both UF and NF, pressure and flowrate were controlled by adjustment of the pump power, the post-column valve, and the permeate side valve. The TMP (P_{TMP}) was calculated as per Eq. 1, where P_1, P_2 and P_3 are the pressures of the feed, retentate and permeate, respectively.

Table 2
Properties of the UF and NF membranes.

Manufacturer	atech	atech	Microdyn Nadir
Membrane type	7/6	7/6	Trisep TS80
Membrane material	ZrO_2	ZrO_2	Thin-film semi-aromatic polyamide
Support material	α–Al_2O_3	α–Al_2O_3	Non-woven polyester
MWCO (Da)	150,000	15,000	150
Surface area (m^2)	0.16	0.16	0.036
Pore width (nm)	1200	400	0.36
Isoelectric point	–	–	at approx. pH 3

$$P_{TMP} = \frac{P_1 + P_2}{2} - P_3 \quad (1)$$

The crossflow velocity (CFV) (v) was calculated by dividing the volumetric flow rate of the feed (Q) by the membrane cross-sectional area (A):

$$v = \frac{Q}{A} \quad (2)$$

2.2. Methods

2.2.1. Experimental procedure

A simplified schematic of the experimental process is depicted in Fig. 2. The first step of the cascade was a solid–liquid separation to remove coarse solids; whereby the FB was filtered through a canvas cloth in a PEW20 pneumatic filter press from the manufacturer GRIFO Macchine Enologiche (Italy). This was done in 30 L batches at a pressure of 3 bar for around 30 min. The filtrate from this stage aggregated and mixed to ensure a consistent starting material.

Though their precise natures and concentrations have not been determined for this FB, natural organic macromolecules, such as proteins and polysaccharides, are known to be present and are thought to contribute to fouling and flux decline in membrane separation. In some studies, however, thermal pretreatment of the feed solution followed by filtration has been shown to be an effective mitigation strategy against fouling [37–40]. Thus, to investigate the possible effects of thermal pretreatments on the filtration performance in this study, half of the basket press filtrate (50 L) was heated to 90 °C under mechanical stirring at 100 rpm over 3.5 h in a custom-built, 130 L jacketed stainless steel open tank reactor. Following the thermal treatment, the FB was allowed to cool overnight before being transferred to 30 L plastic drums for storage at 4 °C.

The UF concentration experiments were performed with 25 kg of the fermentation broth for each of the four alternative paths in the filtration cascade (15 or 150 kDa, thermally treated or not). Filtration was conducted at 40 °C with a TMP of 3 bar and a CFV of 1.7 m s^{-1}, which corresponded to a Reynolds number (Re) of 5510. The experiments were terminated once the volume reduction (VR) had reached approx. 0.9. Before and after each experiment, the filtration system was cleaned with a 1% w/w solution of the alkaline cleaning agent P3-Ultrasil-53 (Ecolab, Germany) followed by a citric acid solution of pH 2.2 (IWV Reagents, Germany; ≥ 99.5%). Cleaning was performed with 7.5 L of each

Table 1
Concentration and properties of the main fatty acids in the fermentation broth.

Carbon atoms	Systematic name	Common name	pKa at 25 °C	Molecular weight (g mol^{-1})	Boiling point (°C)	Solubility at 25 °C (g L^{-1})	Initial FB conc. (g L^{-1})
2	Ethanoic acid	Acetic acid	4.75	60.05	118	miscible	9.32
4	Butanoic acid	Butyric acid	4.81	88.11	164	60.0	2.92
6	Hexanoic acid	Caproic acid	4.84	116.16	205	10.3	2.35
8	Octanoic acid	Caprylic acid	4.89	144.21	239	0.79	0.34

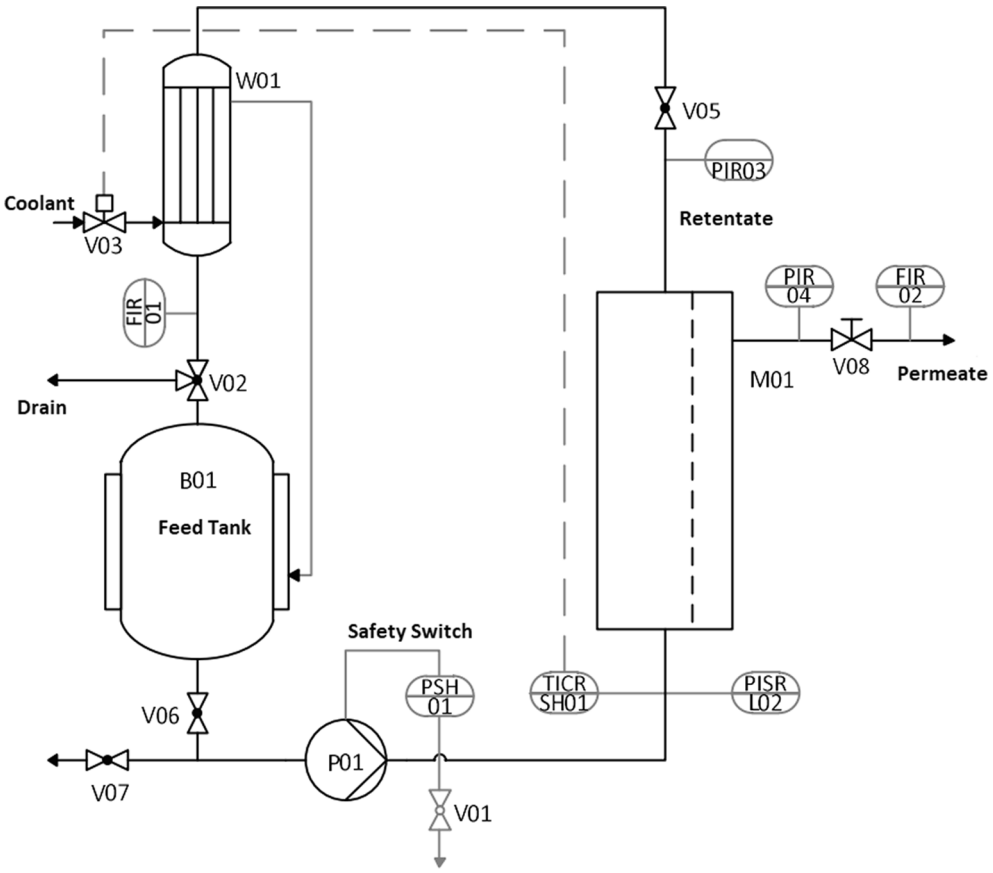

Fig. 1. Process and instrumentation diagram for the PiloMemI filtration unit

solution for 40 min at 40 °C with a TMP of 4 bar and a CFV of 1.7 m s^{-1}. After cleaning, the membrane was flushed with deionized water.

Four NF concentration experiments were performed with 10 kg of UF permeate from one of each of the pretreatment paths (15 or 150 kDa, heated or unheated). The filtration was conducted at 40 °C with a TMP of 30 bar, and a CFV of 1.11 m s^{-1}, which corresponded to a *Re* of 610. The experiments were terminated once the permeate flow rate was <10% of the initial value. The cleaning regime was the same as that in UF, excluding the use of citric acid. After each cleaning cycle, the membrane's $MgSO_4$ retention was measured to monitor changes in solute permeability.

In an attempt to increase permeate flux and *VR*, and to better understand the fouling mechanisms, an additional NF experiment was conducted in diafiltration (DF) mode, which is a feed-dilution technique commonly used for bio-molecule purification [31]. Around 9 kg of thermally treated 15 kDa UF permeate was concentrated to a *VR* of approx. 0.5 under the same conditions as the NF concentration experiments. A volume of deionized water with a mass equal to the collected permeate was then added to the feed tank and the concentration was repeated. This dilution was performed a total of four times (DF volume ratio of 2) before the feed was concentrated to the maximum possible *VR*.

2.2.2. Analysis

FA concentrations (C2-C8) were measured as methyl-ester derivatives with an Agilent 7980 A gas chromatography (GC) system (USA) using a PerkinElmer TurboMatrix HS 110 automated headspace sampler (USA). Esterification was performed directly in the 20 mL glass sample vials by adding 0.5 mL of methanol and 2.5 mL of aqueous sulfuric acid (20% v/v) to 0.3 mL of the sample along with 1.7 mL of deionized water and 1 mL of aqueous 2–methylbutanoic acid (184 mg L^{-1}) as an internal standard. The vials were sealed with crimp caps and stored at 4 °C before being analyzed in triplicate. The GC was operated with a split-splitless injector (220° C), an FID detector and a DB-FFAP column (60 m × 0.5 μm diameter) under nitrogen at an oven temperature of 40° C for 20 min, followed by a gradient of 10 °C min^{-1} for 16 min, then 200 °C for 10 min.

Chemical oxygen demand (COD) measurements were performed by adding a 50 μL aliquot of each sample to pre-prepared LCK 014 cuvettes from the manufacturer Hach (Germany). The assay was heated at 148 °C for 2 h and the absorbance at 605 nm was measured with a DR 3900 UV–Vis Spectrometer (Hach, Germany), the COD was calculated by the instrument.

Determination of dry matter (DM) was performed by weighing between 10 and 60 g of the sample into a ceramic crucible and drying it at 105 °C for 24 h. After cooling in a desiccator, the crucible was weighed again, then the DM was calculated as a weight percentage (w_{DM}) according to Eq. 4, where m_a is the mass of the crucible, m_b the mass of the crucible and sample before drying, and m_c the mass of the crucible and sample after drying.

$$w_{DM} = \frac{(m_c - m_a)}{(m_b - m_a)} \cdot 100\ \% \tag{4}$$

2.2.3. Calculations

Permeate flux (J) was calculated as in Eq. 5 where V_p is the volume of permeate collected in the period t and A is the membrane surface area. Since all phases had a density of 1.0 ± 0.01 g mL^{-1}, mass and volume were taken to be equal in subsequent calculations.

$$J = \frac{V_p}{A \cdot t} \tag{5}$$

From the GC analysis, the observed FA retention (R_{obs}) was calculated as in Eq. 6, where C_p and C_f are the individual species

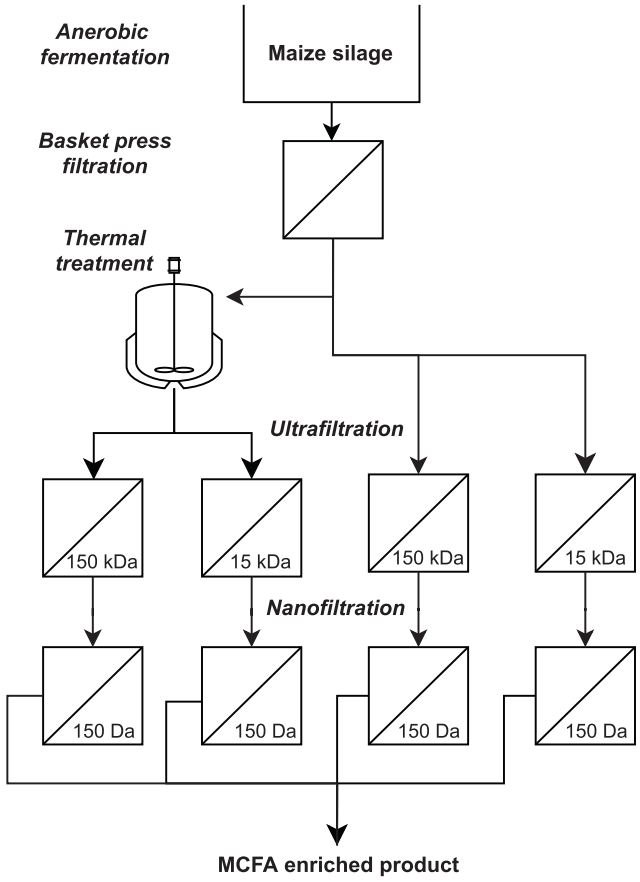

Fig. 2. Simplified process flow diagram of the purification cascade

concentrations in the permeate and feed, respectively.

$$R_{obs} = \left(1 - \frac{C_p}{C_f}\right) \cdot 100\% \quad (6)$$

The *VR* is defined as in Eq. 7, where V_f is the original feed volume and V_p is the permeate volume.

$$VR = \frac{V_p}{V_f} \quad (7)$$

Membrane fouling was also estimated based on pure water flux (PWF) measurements. While there are numerous models and definitions that characterize membrane fouling in different, often overlapping, manners, for this study, the resistance-in-series (RIS) model was used, whereby the total resistance (R_{tot}) is taken to be the sum of the membrane resistance (R_m) and the additional resistance due to membrane fouling (R_f) [32,33]. R_f can be further decomposed according to the origin of the fouling resistance, as in Eq. 8

$$R_f = R_{cp} + R_{g/c} + R_{a/p} + R_{irr} \quad (8)$$

where R_{cp} is due to concentration polarization, $R_{g/c}$ to gel/cake layer development, $R_{a/p}$ to adsorption and removable pore blocking, and R_{irr} to irremovable adsorption and pore blocking.

These parameters were estimated by measuring the PWF with deionized water (<5 µS) before and after each filtration stage. In UF, the PWF was measured at 25 °C with a CFV of 1.7 m s^{-1} over TMPs of 1, 2, 3, and 4 bar. In NF, at 25 °C with a CFV of 1.1 m s^{-1} over TMPs of 10, 20, 30, and 40 bar. The gradient of PWF over the TMP range gave the hydraulic permeability k_w, and the resistance was calculated by substitution into the Darcy equation

$$J_{PWF} = \frac{P_{TMP}}{\eta \cdot R_{tot}} = k_w \cdot P_{TMP} \quad (9)$$

where η is the dynamic viscosity (which, for the FB in this study, was roughly constant and close to that of pure water). In this study, the resistance due to concentration polarization and cake/gel development were not able to be measured. Analysis of fouling was, therefore, based on the additional resistance after rinsing the membrane with water ($R_{a/p} + R_{irr}$), and that remaining after chemical cleaning (R_{irr}).

3. Results and discussion

3.1. Solid-liquid separation

The filter press efficiently removed the coarse solids from the FB and greatly reduced the DM in the liquid phase (Table 3). The low DM content of the filter cake (18.5% w/w), however, amounts to a considerable loss of product in the retained liquid. This process step could be improved by flushing the filter cake with gas or rinsing with process water (e.g., NF permeate), although the latter would increase membrane filtration process volumes and decrease product concentration. Alternatively, since MCFAs are a valuable livestock feed additive, the cost of unrecovered product could be recouped by marketing the filter cake to the agricultural industry.

3.2. Thermal treatment

The results suggest that the thermal treatment of the FB had no significant effect on permeate flux in UF or NF. More detail about the effects of thermal treatment on membrane flux and fouling can be found in sections 3.3 and 3.4. Incidentally, thermal treatment caused a drop of 10% in the COD of the FB which may be the result of heat-accelerated oxidation processes, since COD is a measure of reduction potential (Table 3). A small decrease in the DM of the FB (0.2% w/w) was also measured after heating, although this may lie within the range of experimental error. Visually, no flocculation or precipitation was detected, however, a slight darkening of the filtrate was observed.

3.3. Ultrafiltration

3.3.1. Permeate flux

In each of the four UF concentration experiments, a *VR* of approx. 0.9 was achieved within 160 to 195 min (Fig. 3). The permeate flux remained relatively stable at approx. 55 L m^{-2} h^{-1} until a *VR* of 0.5, after which it began to decline, finally reaching approx. 20 L m^{-2} h^{-1}. This is comparable to other studies with similar filtration systems [34,35]. Of the four UF feeds, the one outlier is the unheated 15 kDa FB, where the flux increased from an initial value of 40.3 L m^{-2} h^{-1} up to a maximum of 55.1 L m^{-2} h^{-1} before declining uniformly with the others. This result is anomalous, since, although there was a small initial flux increase (5 L m^{-2} h^{-1}) for the thermally treated FB on both the 15 and 150 kDa membranes, the initial flux of the unheated FB on the 150 kDa membrane did not increase, remaining constant until a *VR* of 0.5. Such flux increases have been observed in other studies, although the cause remains unclear [36].

The results suggest that the thermal treatment of the FB had no significant effect on permeate flux in UF or NF. While the data is limited, the result appears contrary to other published findings where thermal treatment is associated with enhanced permeate flux due to the heat induced decomposition of natural organic macromolecules [37–40].

The data show that membrane pore size did not have any significant effects on UF permeate flux. While membrane permeability is typically proportional to average pore size, with complex mixtures such as FB it is often not possible to generalize or predict the effect of pore size on permeate flux. Depending on the size of the particles in the feed with

Table 3
Properties of each stream over every stage in the separation cascade, including , where applicable, the sample mean ($\overline{X}$) and standard deviation (s). Recoveries over 100% are a result of experimental uncertainty.

Process Stage	UF membrane	Thermally treated	Phase	Mass	FA recovery		pH	DM		COD	EC
	(kDa)	(Y/N)		kg	%			% w/w		g L^{-1}	mS cm^{-1}
					$\overline{X}$	s		$\overline{X}$	s		
Filter Press	–	–	Permeate	103.9	–	–	6.69	1.95	0.02	60.2	21.3
	–	–	Retentate	29.4			–	18.49	0.12	–	–
Thermal Treatment	–	Y	N/A	51.6	93.8		7.11	1.75	0.02	53.7	21.0
UF	15	N	Permeate	24.8	104.1	3.38	6.80	1.59	0.01	42.6	22.7
			Retentate	2.5			6.97	5.43	0.02	123.2	19.7
		Y	Permeate	21.7	97.8	1.56	7.24	1.99	0.02	40.6	21.4
			Retentate	1.9			7.22	5.27	0.02	121.1	19.7
	150	N	Permeate	22.4	99.3	3.15	6.96	1.70	0.04	46.6	22.7
			Retentate	2.3			7.14	4.70	0.03	121.1	19.7
		Y	Permeate	28.4	107.9	1.89	7.14	2.20	0.09	44.5	20.9
			Retentate	4.9			7.22	5.00	0.01	108.0	19.5
NF	15	N	Permeate	5.8	91.8	1.83	9.80	0.10	0.00	–	3.3
			Retentate	4.6			9.60	3.52	0.04	–	37.9
		Y	Permeate	7.3	89.8	2.90	9.70	0.19	0.01	6.8	5.0
			Retentate	3.0			8.92	4.71	0.03	108.0	44.5
	150	N	Permeate	5.9	89.8	2.74	10.20	0.16	0.01	–	4.3
			Retentate	3.4			9.70	4.20	0.09	–	41.9
		Y	Permeate	6.0	91.1	2.89	9.70	0.16	0.02	–	3.9
			Retentate	3.9			9.10	4.37	0.05	–	40.6

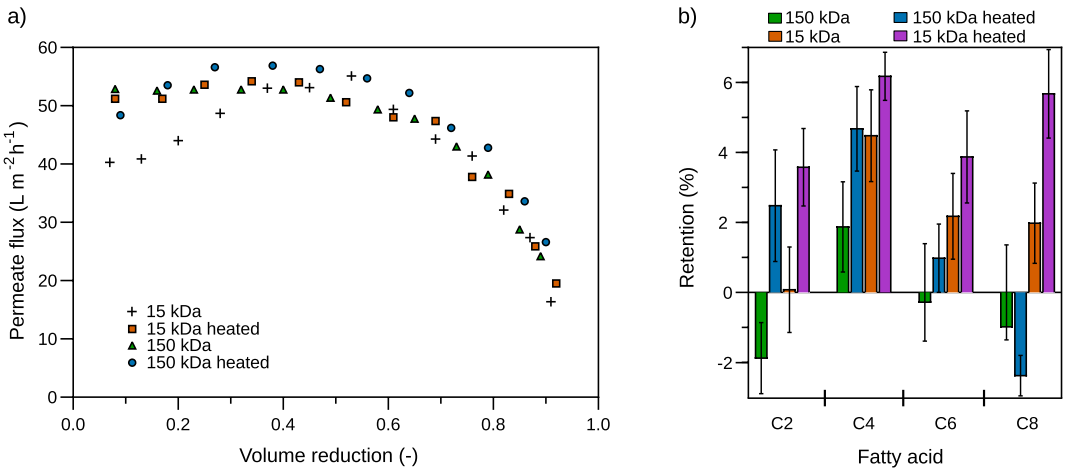

Fig. 3. (a) Permeate flux versus volume reduction), and (b) the observed retention of C2-C8 FAs during the concentration of thermally and not thermally treated pressed maize silage fermentation broth by ultrafiltration.

respect to the pores, flux decline can sometimes increase for larger pored membranes because the foulants can enter the pores and cause internal fouling [35,38].

In this study, however, the flux decline for both the 15 and 150 kDa membranes was uniform, suggesting that the pore size was not a limiting factor for permeate flux. Thus, the dominant resistance is believed to be the development of a gel/cake layer on the membrane surface rather than transport through the membrane itself. As the constitution of the surface layer depends much more on the feed than it does on the nature of the membrane, it follows that the permeate flux was very similar in each of the UF experiments.

3.3.2. Retention

In each UF experiment, the retention of all measured FAs was very low ($\overline{X}$=3.5%, $\sigma < 0.1$), and the effect of pretreatment was negligible (Fig. 3, Table 3). Negative rejections are a result of experimental uncertainty. Such low retention of low-MW FAs was expected for membranes with much larger relative pore sizes. As the UF retentate can likely be recycled back into the fermentation, the 2–6% rejection of FAs in this stage is not considered as a loss of product in the overall process.

On average, the separation resulted in a slight decrease in the density (approx. 10 g L^{-1}) and DM (approx. 0.1% w/w) of the permeate, while the pH was not significantly altered. There were negligible differences between each of the four experiments. The average COD of the UF permeate was 43 g L^{-1}, that of the retentate 118 g L^{-1} (Table 3). The COD of the permeates from the 15 kDa membrane were slightly lower (3 g L^{-1}) than those from the 150 kDa membrane, possibly because more organic macromolecules were separated by the tighter membrane.

3.3.3. Fouling

PWF measurements showed that each filtration cycle caused an additional and substantial increase in the total resistance compared to the virgin membranes (Table 4). The increase in total resistance over two filtration cycles is depicted in (Fig. 4a) for 150 kDa membrane, which is also representative of the trend seen with the 15 kDa membrane. While much of the resistance due to absorption and pore blocking could be removed by chemical cleaning, the resistance of both the 15 and 150 kDa membranes approximately doubled after their first filtration cycles, which could indicate that the cleaning regime was not sufficiently aggressive. These observations could also be the result of a

Table 4
Changes in UF and NF resistances post-rinsing ($R_{a/p}$) and post-cleaning (R_{irr}), expressed as multiples of the respective virgin membrane resistance (R_m).

Membrane	Experimental Cycle 1		Experimental Cycle 2	
	$R_{a/p}/R_m$	R_{irr}/R_m	$R_{a/p}/R_m$	R_{irr}/R_m
150 kDa	5.5	1.9	11.6	3.4
15 kDa (pre-studies)	–	1.7	–	2.9
15 kDa	–	3.6	6.8	3.9
TS80 (1st membrane)	1.5	1.2	1.6	1.3
TS80 (2nd membrane)	1.5	1.3	1.7	1.5

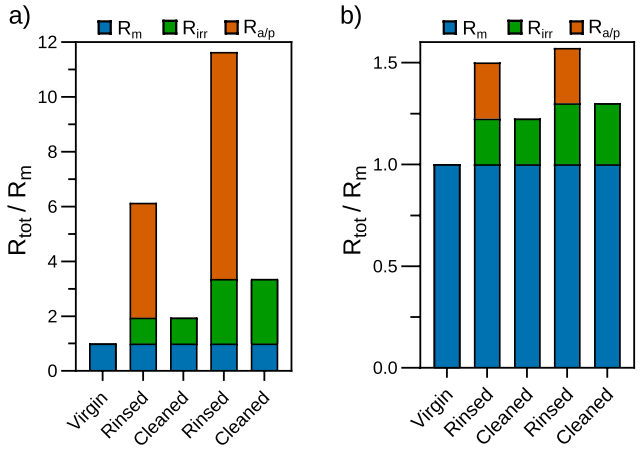

Fig. 4. (a) The ratio of total resistance (R_{tot}) to virgin membrane resistance (R_m) over the course of two filtration cycles for the 150 kDa UF membrane, and (b) the first TS80 NF membrane. $R_{a/p}$ is the additional resistance due to pore blocking and absorption, and R_{irr} is that due to irremovable internal fouling.

normal "wearing in" process, whereby the largest pores become permanently blocked during initial use, resulting in an immediate increase in resistance which then stabilizes over time. This is supported by the fact that the increase in the resistance of the 15 kDa (which was used for additional pre-studies) became much smaller between the third and fourth filtration cycles.

Despite the increasing levels of fouling apparent after rinsing and cleaning neither membrane exhibited a related decrease in FB permeate flux. This observation supports the supposition that the membrane transport was, in these cases, determined predominately by the gel/cake surface layer rather than by the resistance of membrane (or any additional internal fouling).

3.4. Nanofiltration

3.4.1. Permeate flux

In each of the NF concentration experiments, a *VR* of between 0.56 and 0.65 was achieved, and the highest initial permeate fluxes were seen with the UF permeate from the 15 kDa membrane (Fig. 5a). Of the two, the heated 15 kDa UF permeate feed appeared to have the best performance, with an initial flux of 77 L m^{-2} h^{-1} compared to 67 L m^{-2} h^{-1} for the unheated 15 kDa UF permeate feed. It was expected that the combination of thermal treatment and smaller UF pore size would reduce the concentration of NF foulants the most, thus that the heated 15 kDa UF permeate feed would have the highest permeate flux. While the heated 15 kDa UF permeate feed retained the highest flux until near the end of the concentration, the unheated 15 kDa UF permeate feed experienced a more rapid flux decline, and after a *VR* of 0.35 had the lowest flux of all four feeds. Between the heated and unheated feeds from the 150 kDa UF membrane, there was almost no difference in NF flux across the entire experiment. This could be because most of the large organic macromolecules are removed in each UF path, therefore they do not cause fouling in NF and their denaturation would be irrelevant. Unlike in UF where a relatively stable flux persisted until *VR* > 0.6, flux decline in the NF experiments was direct and linear. Despite the rapid decline, the permeate flux in this study compares favorably to that reported for the filtration of a model FB solution with the TS80 membrane (20 L m^{-2} h^{-1}, 30 bar, stirred cell) [41]. Regardless of the initial rate, if permeate flux cannot be sustained over extended periods, the NF stage would likely make the entire process unfeasible. Further research is necessary to determine the exact cause of the flux decline and to develop mitigation strategies.

3.4.2. Retention

In the NF retentate, the final concentration of the C2-C8 FAs was more than double that of the original FB (Table 5), and the observed retentions were between 85% and 95% (Fig. 5b). In NF, surface charge effects are thought to dominate over size exclusion, however, solute retention mechanisms are extremely complex and cannot be properly modelled for mixtures as complex as FB. Nonetheless, such high retentions were expected for these molecules based on electrostatic repulsion, since at the FB's typical pH of >6.8, the FAs are almost entirely deprotonated (pKa ≅ 4.8) and the membrane is negatively charged (IEP ≅ 3). The fact that around 10–15% of the FAs passed

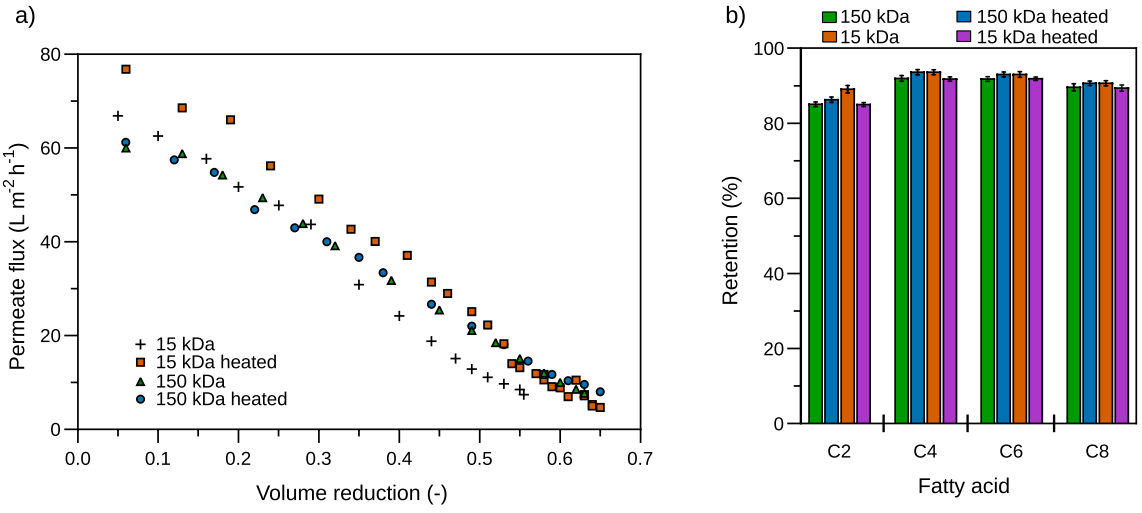

Fig. 5. (a) Permeate flux versus volume reduction and (b) the observed retention of C2-C8 FAs during the concentration of thermally and not thermally treated ultrafiltration permeate from pressed maize silage fermentation broth by nanofiltration

Table 5
Concentration factor, mean concentration (μ) and (where applicable) population standard deviation (σ) of the C2-C8 fatty acids in the fermentation broth (FB), nanofiltration (NF) permeates, and NF retentates.

Fatty acid	FB (g L^{-1})	NF permeate (g L^{-1})		NF retentate (g L^{-1})		Concentration factor
		μ	σ	μ	σ	μ
Ethanoic acid	9.32	1.20	0.14	21.90	1.78	2.35
Butanoic acid	2.92	0.20	0.02	6.78	0.62	2.32
Hexanoic acid	2.35	0.17	0.01	5.39	0.45	2.29
Octanoic acid	0.34	0.03	0.00	0.75	0.05	2.20

through the membrane could possibly be attributed to reductions in electrostatic repulsion caused by the association of positively charged solutes to the membrane surface or the FA molecules.

Although typically a non-dominant mechanism, size exclusion can be an important factor in membrane selectivity. In this case, the MWCO of the membrane (150 Da) was only marginally greater than the MW range of the FAs (60–144 Da). The differences in retention between the FAs could, thus, arise from competition between convective and electrostatic transport mechanisms. The declining retention from C4-C8 could be due to the decrease in hydrophilicity and charge density with increasing MW, allowing less the electrostatically hindered molecules to permeate more easily, despite their larger size. In contrast, although ethanoic acid has the greatest charge density, its relatively small size could have meant that transport was dominated by convection mechanisms. The retention of ethanoic acid here was higher than that reported in a study with the TS80 membrane using model solutions at a similar pH [41]. In that case, the average retention of ethanoic acid was only 46%, possibly due to a lower ionic strength or the absence of membrane fouling, which can reduce the effective pore size.

Additionally, the NF separation resulted in, on average, a 0.5-unit reduction in the pH of the retentate and a tenfold increase in electrical conductivity compared to the permeate (Table 3). The pH of the NF feed was also observed to increase by approx. 1–2 pH units after four weeks of storage at 4 °C. The COD of the permeate was reduced to 6.8 g L^{-1}, compared to 108 g L^{-1} in the retentate and 40 g L^{-1} in the feed. This is expected, as many of the acids, organic molecules, and divalent salts were retained by the membrane. The NF permeate was colorless and had a strong ammonia-like odor, whereas the retentate had clear, dark brown color and an odor reminiscent of goats—characteristic of C6 and C8 FAs.

3.4.3. Fouling

The TS80 membranes demonstrated a very similar increase in resistance (approx. 40%) over the two filtration cycles in this study (Fig. 4b). This relatively small increase in irremovable membrane resistance is likely not the main driver of the flux decline seen in the NF. The development of a temporary gel/cake layer and the occurrence of concentration polarization (both at the membrane surface layer), are expected to be much more important factors. More detailed fouling studies would be necessary to precisely elucidate the dominant modes of fouling in this case.

Additionally, the $MgSO_4$ retention of both membranes decreased by approx. 5% with each filtration cycle, although a deterioration in membrane integrity was not suggested by the FA retention data. During the third cleaning cycle of the first membrane, however, a rupture was evident in the extreme decrease in $MgSO_4$ retention (from 90% to 40%) and the increase in permeability.

As in UF, it appears that the cleaning regime is insufficient for the removal of accumulated membrane foulants between filtration cycles. Unlike UF, however, many NF membranes are easily damaged by aggressive chemical cleaning, which makes foulant removal particularly challenging. Ideally, membrane foulants should be removed before NF, though the pretreatment in this filtration cascade was apparently inadequate. While the identities of the NF foulants are yet to be confirmed, humic substances are indicated, since they are found in the feedstock and are known to cause irreversible flux decline in membrane filtration [40,42]. Although these substances are particularly incalcitrant, it may be possible to remove them from the NF feed by using a UF membrane with a lower MWCO (e.g., 1 kDa or 5 kDa).

3.5. Diafiltration

3.5.1. Permeate flux

The effect of DF on permeate flux was generally negligible, though, toward the end of each concentration ($VR > 0.5$), a small flux increase (4 L m^{-2} h^{-1}) was observed after the third and fourth dilutions (Fig. 6). This minor benefit comes, however, at a substantial time cost: the DF took 1200 min to reach a *VR* of 0.65, compared to 360 min for the standard NF concentrations.

3.5.2. Retention

The dilution by diafiltration caused a decrease in the effective retention for butanoic acid (11.2%), hexanoic acid (14.2%), and octanoic acid (11.9%). The retention of ethanoic acid was most markedly reduced (32.8%), likely a result of its smaller size and relatively higher polarity. The reduction in the retention of the FAs is unsurprising as the diafiltration factor was 2, which amounted to a total permeate volume of 24 kg compared to approx. 6 kg for the standard NF. DF appears to offer no benefit given the substantial additional costs in terms of yield, resources, and time.

4. Conclusion

A filtration cascade was developed to recover MCFAs from maize silage FB. The process achieved effective solid–liquid separation and the NF membrane retained >90% of MCFAs. Pretreatment variations (thermal treatment and UF pore size) appear to have had a negligible effect on flux and MCFA retention, though repetition is required to confirm this. Membrane fouling, however, caused immediate flux decline that limited the final MCFA concentration in each NF experiment and was not improved by diafiltration. While not a highly-concentrated product, the NF retentate is clarified and was enriched by a factor of 2.3 compared to the feed stock, having an average MCFA concentration of 12.9 g L^{-1} (C4-C8). The process, overall, had an average MCFA recovery of 84%. Thus, while further development is clearly necessary to mitigate fouling, when combined with an additional downstream purification stage, the present process could be an effective step in the sustainable production of MCFAs.

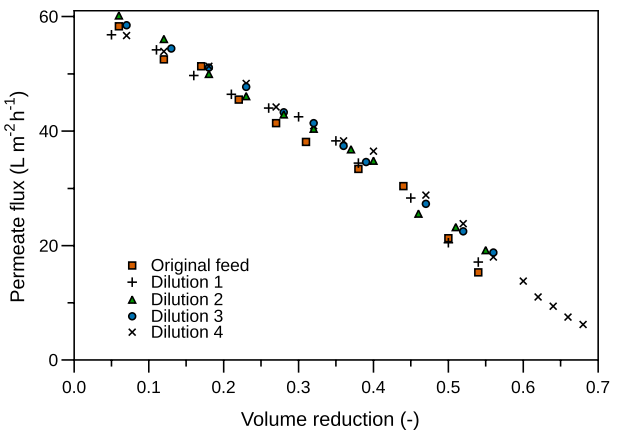

Fig. 6. Permeate flux versus volume reduction for the diafiltration during nanofiltration of ultrafiltration (15 kDa) permeate of thermally-treated fermentation broth

CRediT authorship contribution statement

Stewart Charles McDowall: Investigation, Data curation, Writing – original draft, Writing – review & editing, Visualization. **Maria Braune:** Resources, Writing – review & editing, Supervision, Project administration, Funding acquisition. **Roy Nitzsche:** Conceptualization, Methodology, Resources, Writing – review & editing, Supervision, Project administration.

Declaration of Competing Interest

The authors declare that they have no known competing financial interests or personal relationships that could have appeared to influence the work reported in this paper.

Acknowledgements

We thank Heike Sträube from the Helmholtz Environmental Research Center (UFZ, Leipzig) for providing the fermentation broth used in this study. This research was funded by the German Federal Ministry of Education and Research (BMBF) and by the German Federal Ministry of Food and Agriculture (BMEL) under the grant number 031B0389.

Appendix A. Supplementary material

Supplementary data to this article can be found online at https://doi.org/10.1016/j.seppur.2021.120430.

References

[1] J. Sherwood, The significance of biomass in a circular economy, Bioresour. Technol. 300 (2020) 122755, https://doi.org/10.1016/j.biortech.2020.122755.
[2] Agriculture Commission at the German Federal Environment Agency (Kommission Landwirtschaft beim Umweltbundesamt), On the Future of Biogas Generation and Utilisation, Dessau-Roßlau, 2013. https://www.umweltbundesamt.de/sites/default/files/medien/376/publikationen/on_the_future_of_biogas_generation_and_utilisation_klu.pdf.
[3] S. Theuerl, C. Herrmann, M. Heiermann, P. Grundmann, N. Landwehr, U. Kreidenweis, A. Prochnow, The future agricultural biogas plant in Germany: A vision, Energies. 12 (2019) 396, https://doi.org/10.3390/en12030396.
[4] Q. Wu, X. Bao, W. Guo, B. Wang, Y. Li, H. Luo, H. Wang, N. Ren, Medium chain carboxylic acids production from waste biomass: Current advances and perspectives, Biotechnol. Adv. 37 (5) (2019) 599–615, https://doi.org/10.1016/j.biotechadv.2019.03.003.
[5] E. Meijaard, T.M. Brooks, K.M. Carlson, E.M. Slade, J. Garcia-Ulloa, D.L.A. Gaveau, J.S.H. Lee, T. Santika, D. Juffe-Bignoli, M.J. Struebig, S.A. Wich, M. Ancrenaz, L. P. Koh, N. Zamira, J.F. Abrams, H.H.T. Prins, C.N. Sendashonga, D. Murdiyarso, P. R. Furumo, N. Macfarlane, R. Hoffmann, M. Persio, A. Descals, Z. Szantoi, D. Sheil, The environmental impacts of palm oil in context, Nat. Plants 6 (12) (2020) 1418–1426, https://doi.org/10.1038/s41477-020-00813-w.
[6] P. Stamatopoulou, J. Malkowski, L. Conrado, K. Brown, M. Scarborough, Fermentation of organic residues to beneficial chemicals: A review of medium-chain fatty acid production, Processes. 8 (2020) 1–25, https://doi.org/10.3390/pr8121571.
[7] M. Venkateswar Reddy, G. Kumar, G. Mohanakrishna, S. Shobana, R.I. Al-Raoush, Review on the production of medium and small chain fatty acids through waste valorization and CO2 fixation, Bioresour. Technol. 309 (2020) 123400, https://doi.org/10.1016/j.biortech.2020.123400.
[8] J. Chwialkowska, A. Duber, R. Zagrodnik, F. Walkiewicz, M. Łężyk, P. Oleskowicz-Popiel, Caproic acid production from acid whey via open culture fermentation – Evaluation of the role of electron donors and downstream processing, Bioresour. Technol. 279 (2019) 74–83, https://doi.org/10.1016/j.biortech.2019.01.086.
[9] H. Kim, O. Choi, B.S. Jeon, W.-S. Choe, B.-I. Sang, Impact of feedstocks and downstream processing technologies on the economics of caproic acid production in fermentation by Megasphaera elsdenii T81, Bioresour. Technol. 301 (2020) 122794, https://doi.org/10.1016/j.biortech.2020.122794.
[10] W.d.A. Cavalcante, R.C. Leitão, T.A. Gehring, L.T. Angenent, S.T. Santaella, Anaerobic fermentation for n-caproic acid production: A review, Process Biochem. 54 (2017) 106–119, https://doi.org/10.1016/j.procbio.2016.12.024.
[11] K.L. Wasewar, D.Z. Shende, Reactive extraction of caproic acid using tri-n-butyl phosphate in hexanol, octanol, and decanol, J. Chem. Eng. Data 56 (2) (2011) 288–297, https://doi.org/10.1021/je100974f.
[12] K.L. Wasewar, D.Z. Shende, Extraction of caproic acid using tri- n -butyl phosphate in benzene and toluene at 301 K, J. Chem. Eng. Data 55 (9) (2010) 4121–4125, https://doi.org/10.1021/je100337m.
[13] S. Ge, J.G. Usack, C.M. Spirito, L.T. Angenent, Long-Term n-Caproic Acid Production from Yeast-Fermentation Beer in an Anaerobic Bioreactor with Continuous Product Extraction, Environ. Sci. Technol. 49 (13) (2015) 8012–8021, https://doi.org/10.1021/acs.est.5b00238.
[14] L.A. Kucek, M. Nguyen, L.T. Angenent, Conversion of L-lactate into n-caproate by a continuously fed reactor microbiome, Water Res. 93 (2016) 163–171, https://doi.org/10.1016/j.watres.2016.02.018.
[15] J. Xu, J.J.L. Guzman, S.J. Andersen, K. Rabaey, L.T. Angenent, In-line and selective phase separation of medium-chain carboxylic acids using membrane electrolysis, Chem. Commun. 51 (31) (2015) 6847–6850.
[16] S. Aghapour Aktij, A. Zirehpour, A. Mollahosseini, M.J. Taherzadeh, A. Tiraferri, A. Rahimpour, Feasibility of membrane processes for the recovery and purification of bio-based volatile fatty acids: A comprehensive review, J. Ind. Eng. Chem. 81 (2020) 24–40, https://doi.org/10.1016/j.jiec.2019.09.009.
[17] S. Aydin, H. Yesil, A.E. Tugtas, Recovery of mixed volatile fatty acids from anaerobically fermented organic wastes by vapor permeation membrane contactors, Bioresour. Technol. 250 (2018) 548–555, https://doi.org/10.1016/j.biortech.2017.11.061.
[18] H. Yesil, B. Calli, A.E. Tugtas, A hybrid dry-fermentation and membrane contactor system: Enhanced Volatile Fatty Acid (VFA) production and recovery from organic solid wastes, Water Res. 192 (2021), 116831, https://doi.org/10.1016/j.watres.2021.116831.
[19] P.M. Doran, Bioprocess Engineering Principles, Elsevier (2013), https://doi.org/10.1016/C2009-0-22348-8.
[20] A. Figoli, A. Cassano, A. Basile, Membrane Technologies for Biorefining, Woodhead Publishing; Elsevier (2016), https://doi.org/10.1016/C2014-0-03660-X.
[21] P. Khunnonkwao, K. Jantama, S. Kanchanatawee, S. Galier, H., Roux-de Balmann, A two steps membrane process for the recovery of succinic acid from fermentation broth, Sep. Purif. Technol. 207 (2018) 451–460, https://doi.org/10.1016/j.seppur.2018.06.056.
[22] H.D. Lee, M.Y. Lee, Y.S. Hwang, Y.H. Cho, H.W. Kim, H.B. Park, Separation and Purification of Lactic Acid from Fermentation Broth Using Membrane-Integrated Separation Processes, Ind. Eng. Chem. Res. 56 (29) (2017) 8301–8310, https://doi.org/10.1021/acs.iecr.7b02011.
[23] V.S. Bisaria, A. Kondo, Bioprocessing of Renewable Resources to Commodity Bioproducts, Wiley, Hoboken New Jersey (2014), https://doi.org/10.1002/9781118845394.
[24] M.P. Zacharof, S.J. Mandale, P.M. Williams, R.W. Lovitt, Nanofiltration of treated digested agricultural wastewater for recovery of carboxylic acids, J. Cleaner Prod. 112 (2016) 4749–4761, https://doi.org/10.1016/j.jclepro.2015.07.004.
[25] M. Atasoy, I. Owusu-Agyeman, E. Plaza, Z. Cetecioglu, Bio-based volatile fatty acid production and recovery from waste streams: Current status and future challenges, Bioresour. Technol. 268 (2018) 773–786, https://doi.org/10.1016/j.biortech.2018.07.042.
[26] T. Jänisch, S. Reinhardt, U. Pohsner, S. Böringer, R. Bolduan, J. Steinbrenner, H. Oechsner, Separation of volatile fatty acids from biogas plant hydrolysates, Sep. Purif. Technol. 223 (2019) 264–273, https://doi.org/10.1016/j.seppur.2019.04.066.
[27] C. Bellona, J.E. Drewes, The role of membrane surface charge and solute physico-chemical properties in the rejection of organic acids by NF membranes, J. Membr. Sci. 249 (1-2) (2005) 227–234, https://doi.org/10.1016/j.memsci.2004.09.041.
[28] H. Sträuber, F. Bühligen, S. Kleinsteuber, M. Dittrich-Zechendorf, Carboxylic acid production from ensiled crops in anaerobic solid-state fermentation - trace elements as pH controlling agents support microbial chain elongation with lactic acid, Eng. Life Sci. 18 (7) (2018) 447–458, https://doi.org/10.1002/elsc.201700186.
[29] J. Lambrecht, N. Cichocki, F. Schattenberg, S. Kleinsteuber, H. Harms, S. Müller, H. Sträuber, Key sub-community dynamics of medium-chain carboxylate production, Microb. Cell Fact. 18 (2019) 92, https://doi.org/10.1186/s12934-019-1143-8.
[30] S.C. McDowall, Development of a Membrane Filtration Cascade for the Recovery of Biomass-Derived Medium-Chain Fatty Acids, 2020. https://doi.org/10.13140/RG.2.2.30129.10082.
[31] F. Lipnizki, Membrane Processes for the Production of Bulk Fermentation Products, Membrane Technology, in: Membrane Technology, Elsevier, 2010, pp. 121–153, https://doi.org/10.1016/B978-1-85617-632-3.00007-0.
[32] G. di Bella, D. di Trapani, A brief review on the resistance-in-series model in membrane bioreactors (MBRs), Membranes. 9 (2019) 24, https://doi.org/10.3390/membranes9020024.
[33] R. Nitzsche, J. Köchermann, A. Gröngröft, M. Kraume, Nanofiltration of Organosolv Hemicellulose Hydrolyzate: Influence of Hydrothermal Pretreatment and Membrane Characteristics on Filtration Performance and Fouling, Ind. Eng. Chem. Res. 60 (2) (2021) 916–930, https://doi.org/10.1021/acs.iecr.0c03256.
[34] P.P. Ravi, W. Merkle, M. Tuczinski, F. Saravia, H. Horn, A. Lemmer, Integration of membrane filtration in two-stage anaerobic digestion system: Specific methane yield potentials of hydrolysate and permeate, Bioresour. Technol. 275 (2019) 138–144, https://doi.org/10.1016/j.biortech.2018.12.043.
[35] F. Waeger, T. Delhaye, W. Fuchs, The use of ceramic microfiltration and ultrafiltration membranes for particle removal from anaerobic digester effluents, Sep. Purif. Technol. 73 (2) (2010) 271–278, https://doi.org/10.1016/j.seppur.2010.04.013.
[36] J. Luo, W. Cao, L. Ding, Z. Zhu, Y. Wan, M.Y. Jaffrin, Treatment of dairy effluent by shear-enhanced membrane filtration: The role of foulants, Sep. Purif. Technol. 96 (2012) 194–203, https://doi.org/10.1016/j.seppur.2012.06.009.

[37] N. Hilal, O.O. Ogunbiyi, N.J. Miles, R. Nigmatullin, Methods employed for control of fouling in MF and UF membranes: A comprehensive review, Sep. Sci. Technol. 40 (10) (2005) 1957–2005, https://doi.org/10.1081/SS-200068409.
[38] M. Gryta, Fouling in direct contact membrane distillation process, J. Membr. Sci. 325 (1) (2008) 383–394, https://doi.org/10.1016/j.memsci.2008.08.001.
[39] M. Kasmi, M. Hamdi, I. Trabelsi, Processed milk waste recycling via thermal pretreatment and lactic acid bacteria fermentation, Environmental Science and Pollution, Research. 24 (15) (2017) 13604–13613, https://doi.org/10.1007/s11356-017-8932-6.
[40] A. Alkhatib, M.A. Ayari, A.H. Hawari, Fouling mitigation strategies for different foulants in membrane distillation, Chemical Engineering and Processing - Process Intensification. 167 (2021) 108517, https://doi.org/10.1016/j.cep.2021.108517.
[41] J.Y. Law, A.W. Mohammad, Separation of succinate from organic acid salts using nanofiltration membranes, Chemical, Engineering Transactions. 56 (2017) 1705–1710, https://doi.org/10.3303/CET1756285.
[42] F. Zhao, Y. Zhang, H. Chu, S. Jiang, Z. Yu, M. Wang, X. Zhou, J. Zhao, A uniform shearing vibration membrane system reducing membrane fouling in algae harvesting, J. Cleaner Prod. 196 (2018) 1026–1033, https://doi.org/10.1016/j.jclepro.2018.06.089.